

Electronic Supporting Information

Metals coordination in the high-temperature leaching of NdFeB magnets with the ionic liquid betainium bis(trifluoromethylsulfonyl)imide

Martina Orefice,^a Koen Binnemans,^{a*} Tom Vander Hoogerstraete,^a

a. KU Leuven, Department of Chemistry, Celestijnenlaan 200F, 3001 Heverlee (Belgium). *Corresponding author, e-mail: koen.binnemans@kuleuven.be

Synthesis and stability of [Hbet][Tf₂N]

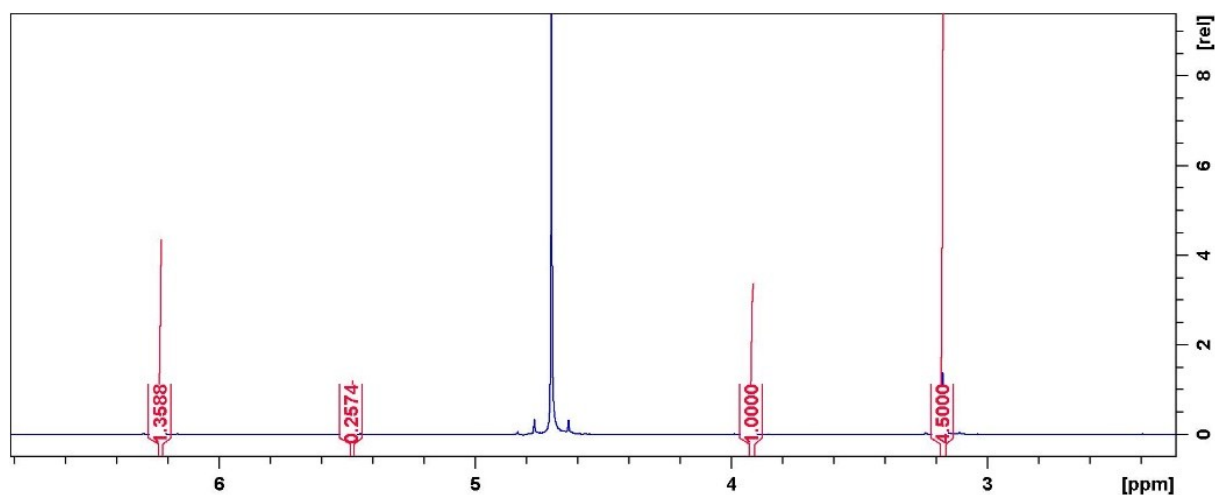


Figure S1 – ¹H NMR spectrum of the [Hbet][Tf₂N] with integrated peaks. The peaks at ~3.2 ppm and ~3.9 ppm correspond to the alkyl groups, on the N and on the α-C, respectively.

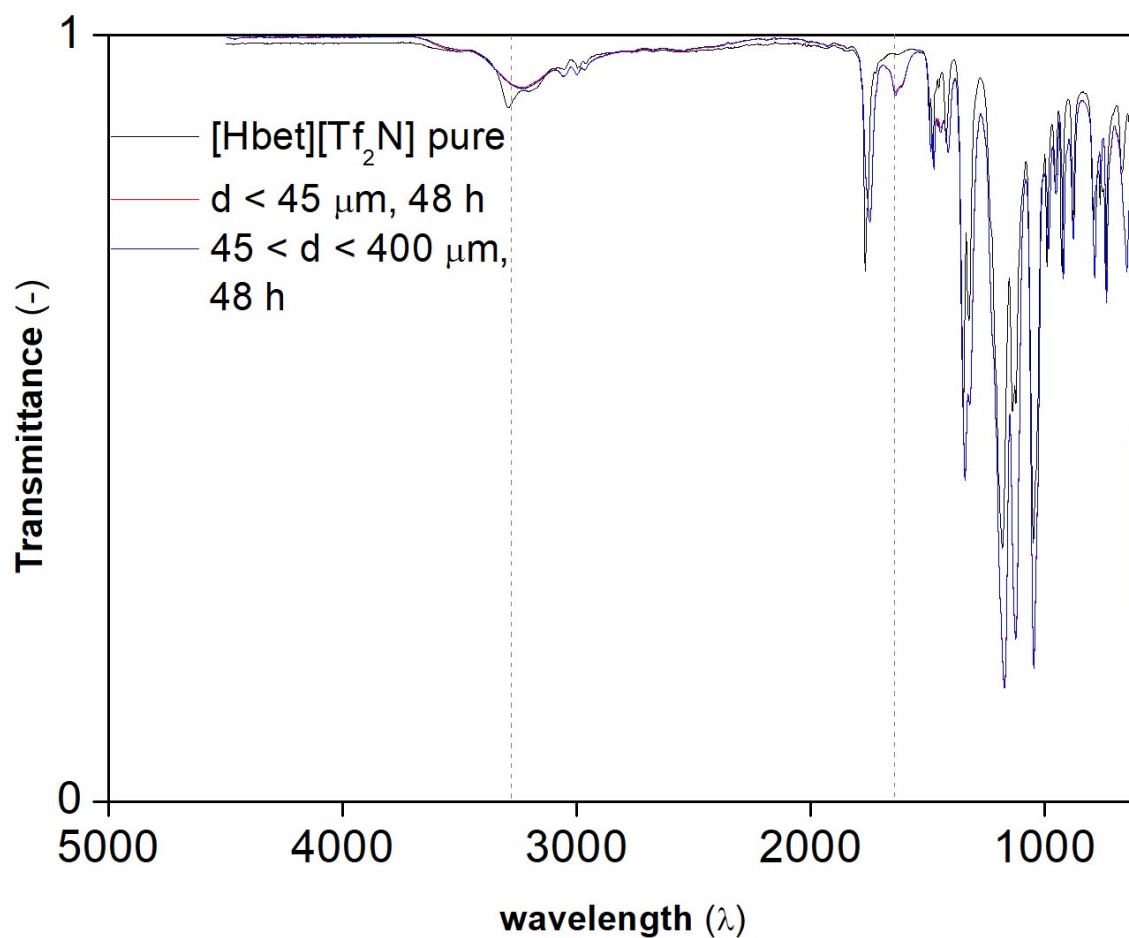


Figure S2 – FTIR spectra of the pure, solid [Hbet][Tf₂N] and of 48 h leachate with particle fractions below 45 μm and between 45 and 400 μm.

Characterization and pre-treatment of the solid material

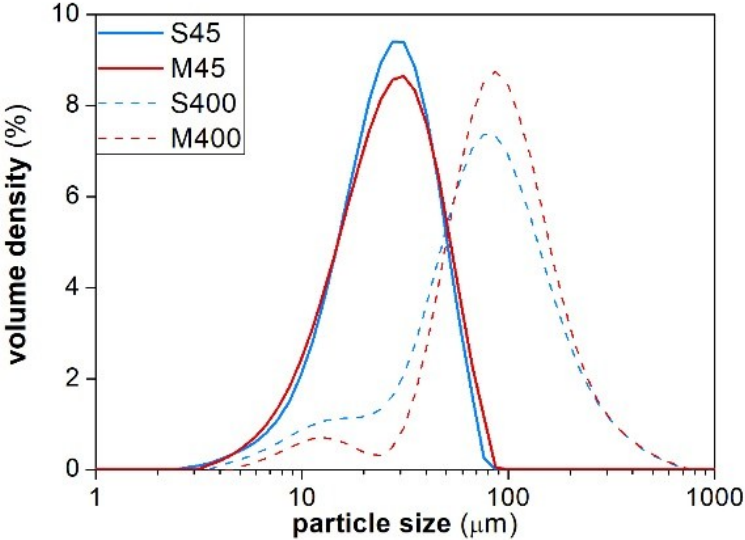


Figure S3 - Probability distribution function of magnets (M) and scrap (S). 45 and 400 refer to the upper limit of the fraction (in microns).

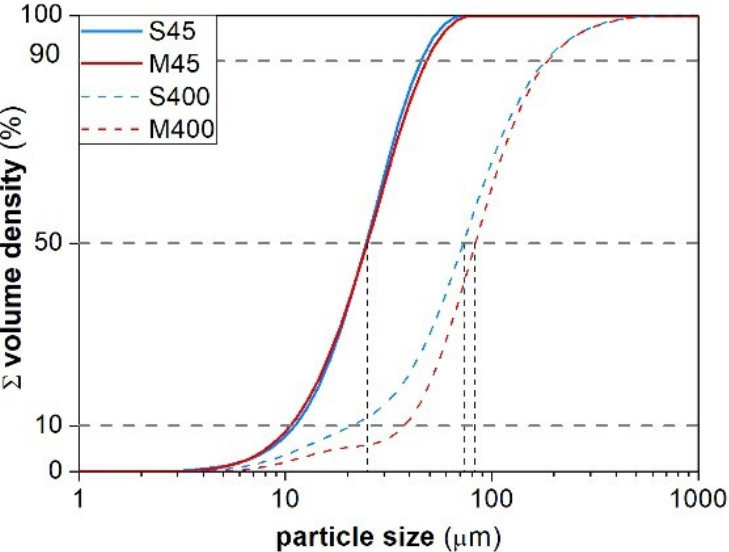


Figure S4 - Cumulative distribution function of magnets (M) and scrap (S). 45 and 400 refer to the limit of the fraction (in microns). The d_{50} diameter is marked for all the curves, while for the d_{10} and d_{90} diameters only the guideline is reported for clarity.

Table S1 - d_{10} , d_{50} and d_{90} of the NdFeB scrap and magnet fractions below 45 μm , S45 and M45, and between 45 and 400 μm , S400 and M400.

Fraction	d_{10}	d_{50}	d_{90}
	(μm)		
S45	12.6	27.9	51.5
M45	11.9	28.2	54.9
S400	23.6	82.5	205
M400	42.5	94.5	211

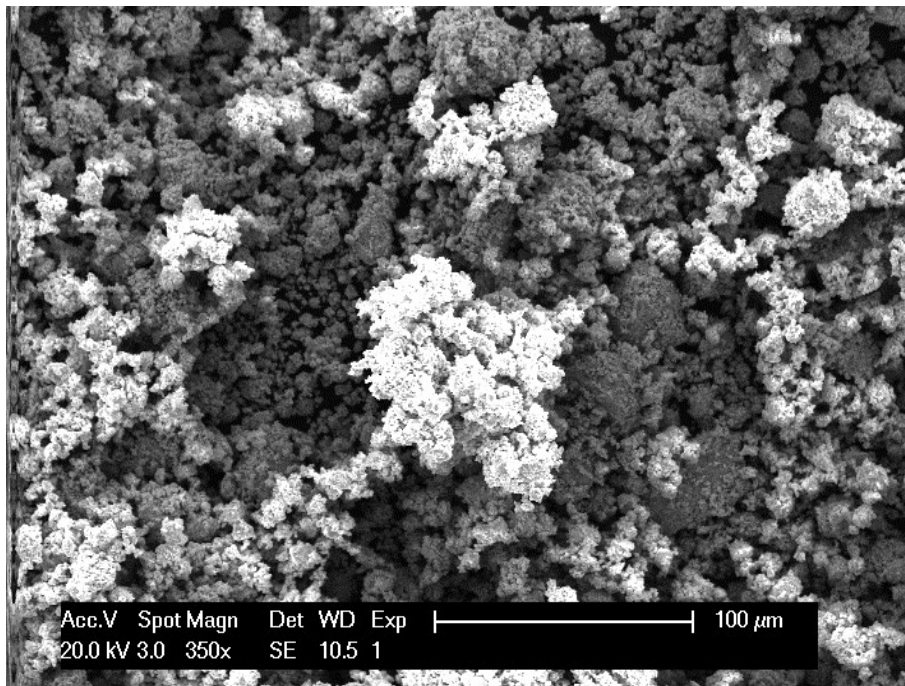


Figure S5 – SEM image (magnification 350 \times) of the non-roasted magnet, after crushing and milling.

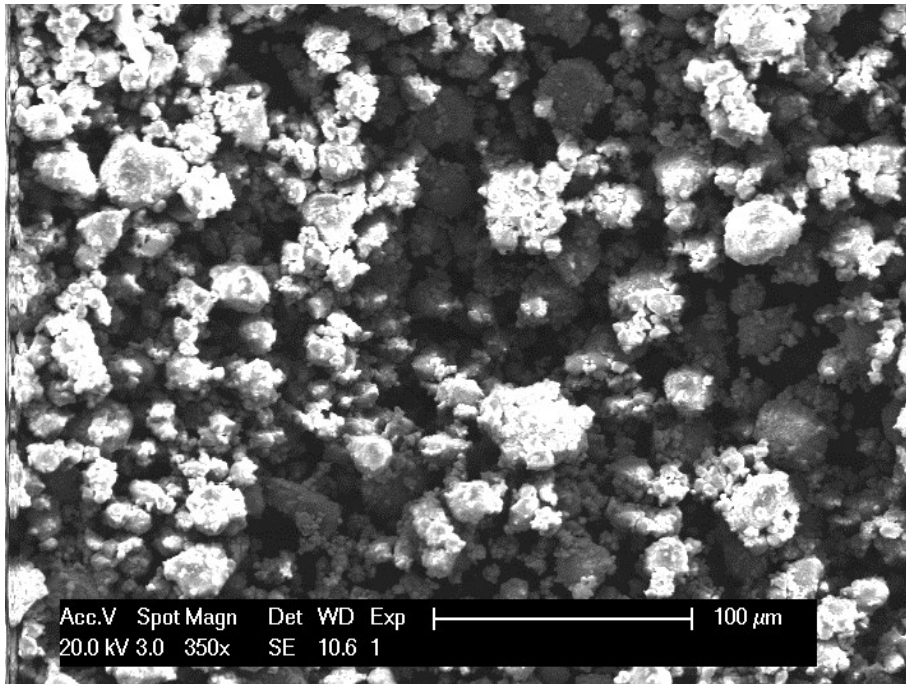


Figure S6– SEM image (magnification 350×) of the roasted magnet, after crushing and milling. There is no distinct difference in the morphology before and after the roasting process.

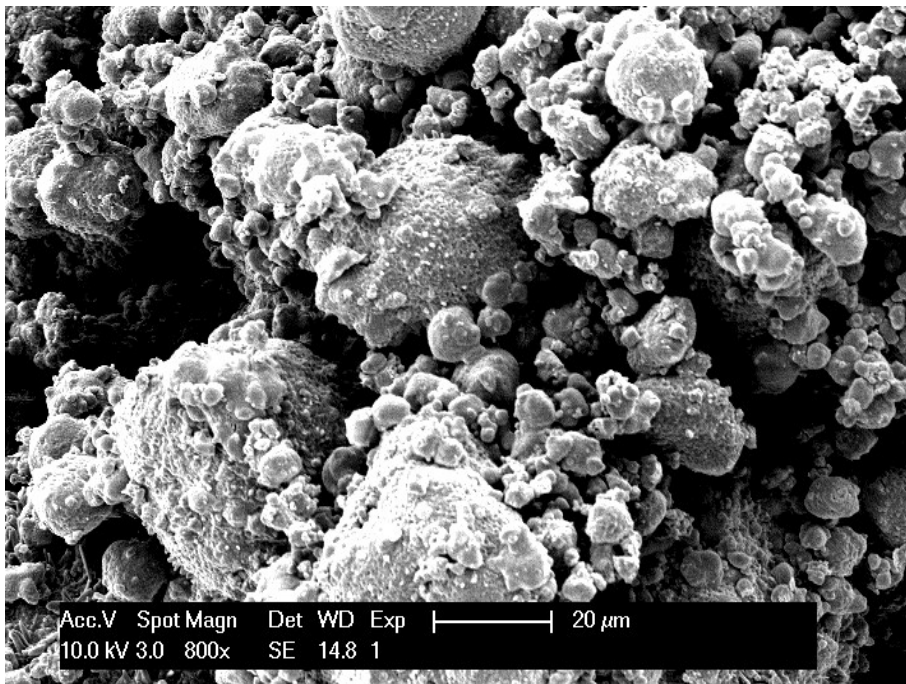


Figure S7– SEM image (magnification 800×) of the roasted magnet, after crushing and milling. Polydispersity of the distribution is observable and especially the particles are clearly distinguishable. No phenomena of cold-sintering occurred during the milling process, despite the high milling energies.

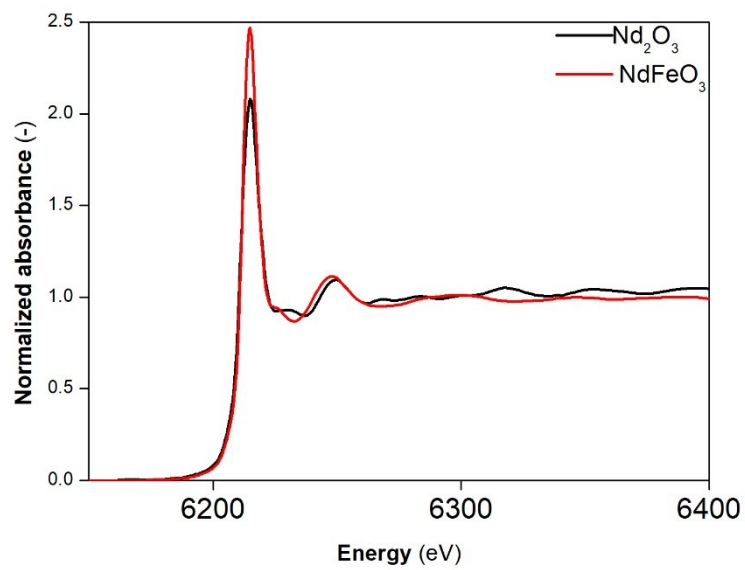


Figure S8 – XANES function fitted for the compound NdFeO_3 compared to that of Nd_2O_3 .

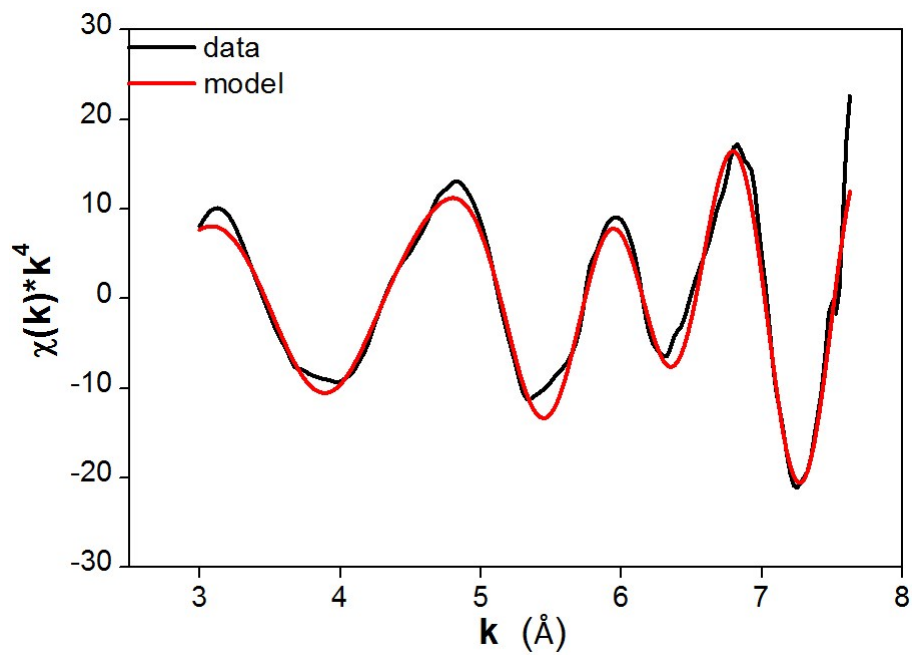


Figure S9 – EXAFS function for the NdFeO_3 compared to the model.

Table S2 – Elemental composition of the NdFeB dross from scrap casting production (in wt.%) determined with ICP-OES.

Element	Composition (wt.%)
Fe	59.21
Nd	33.21
Dy	4.89
Pr	0.54
Co	1.93
Cu	0.03
Mn	0.01
Al	0.02
B	0.17

compositions normalised to 100%

Table S3 - Mineral composition determined by quantitative XRD of NdFeB dross from scrap casting production.

NdFeB dross	
Compound	wt.%
Nd ₂ O ₃	0.18
NdBO ₃	4.09
NdFeO ₃	33.41
Fe ₂ O ₃	62.33

Table S4 - d_{10} , d_{50} and d_{90} of fractions of the NdFeB dross from scrap casting below 45 μm , S45 and M45, and between 45 and 400 μm , S400 and M400.

Fraction	d_{10}	d_{50}	d_{90}
	(μm)		
D45	10.3	21.5	43.1
D400	12.8	33.1	110

Plots of the particles size distribution were considered not significant due to the use of the solid above only for a proof-of-concept test.

Leaching test

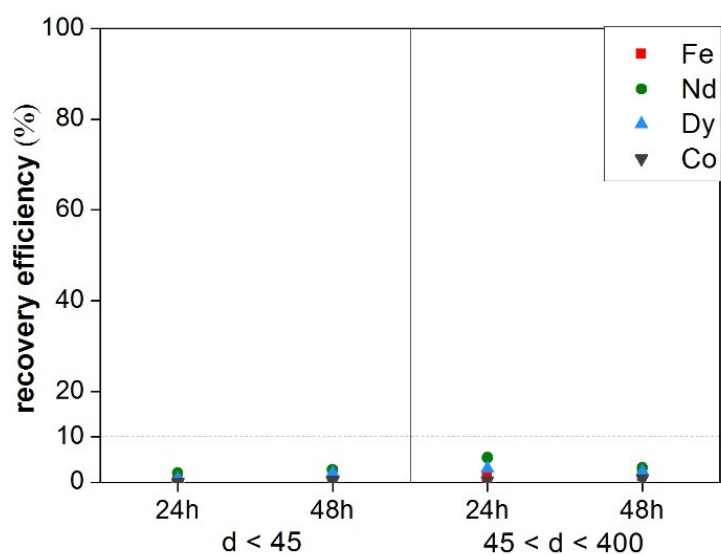


Figure S10 – Recovery efficiency (%) of Fe(III), Nd(III), Dy(III) and Co(II) from the scrap for as a function of the time and the particle size.

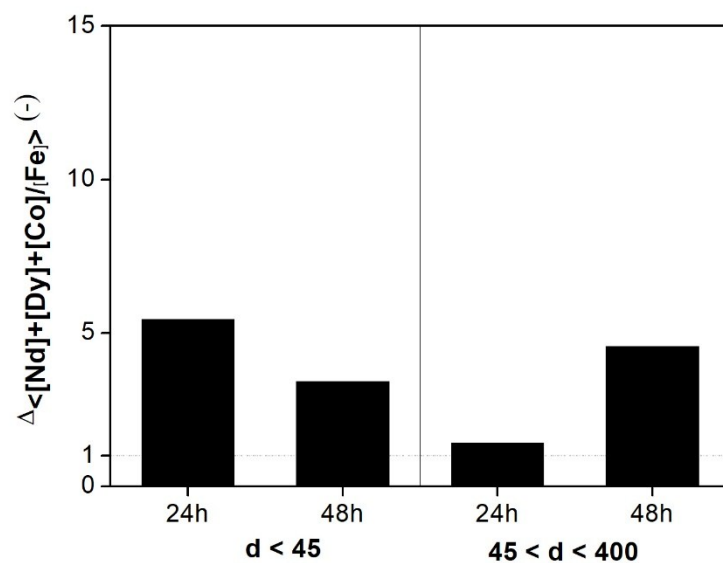


Figure S11 – Relative selectivity of the leaching process for the scrap as a function of the time and the particle size. A reference value of 1 to the initial ratio is pointed out for comparison.

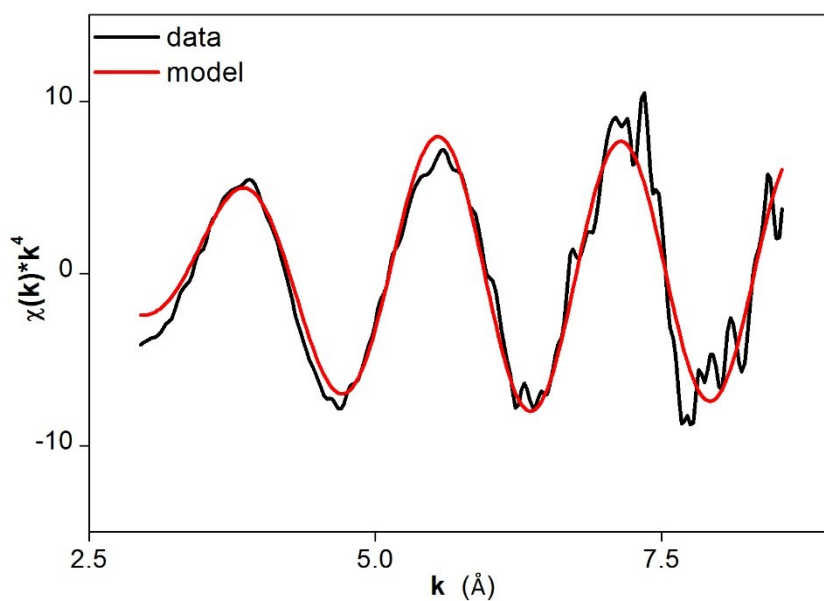


Figure S12 - EXAFS function and model for the Pr_6O_{11} in dry [Hbet][Tf₂N].

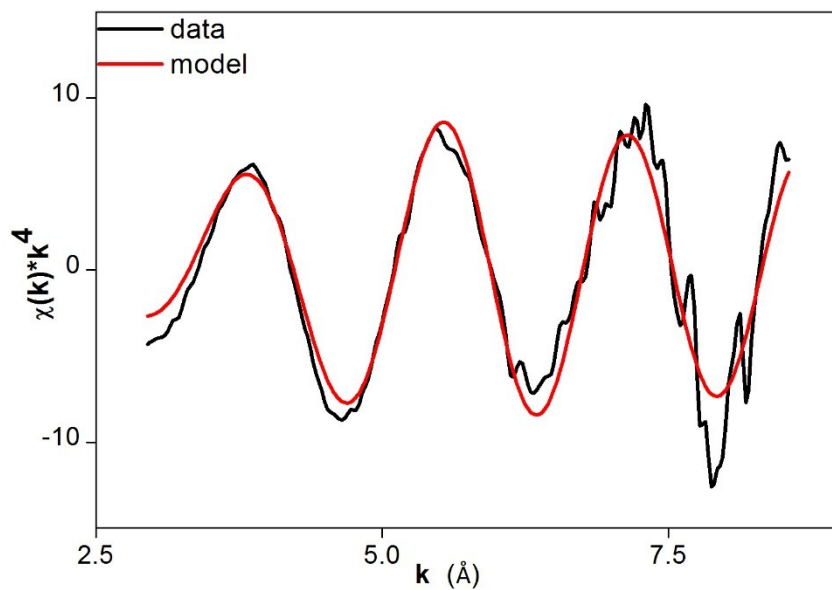


Figure S13- EXAFS function and model for the Pr_6O_{11} in water-saturated $[\text{Hbet}][\text{Tf}_2\text{N}]$.

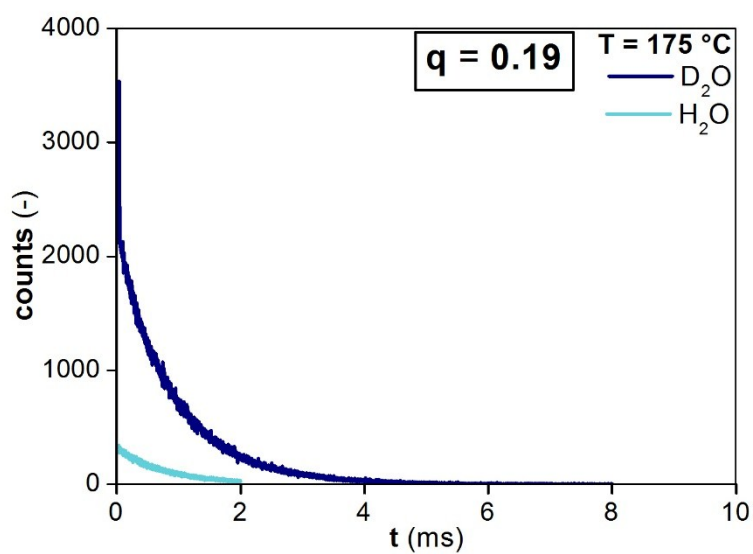


Figure S14 – Emission decay curves at room temperature of Eu^{3+} dissolved at 175 °C in dry $[\text{Dbet}][\text{Tf}_2\text{N}]$ and dry $[\text{Hbet}][\text{Tf}_2\text{N}]$. $q = 0.19$

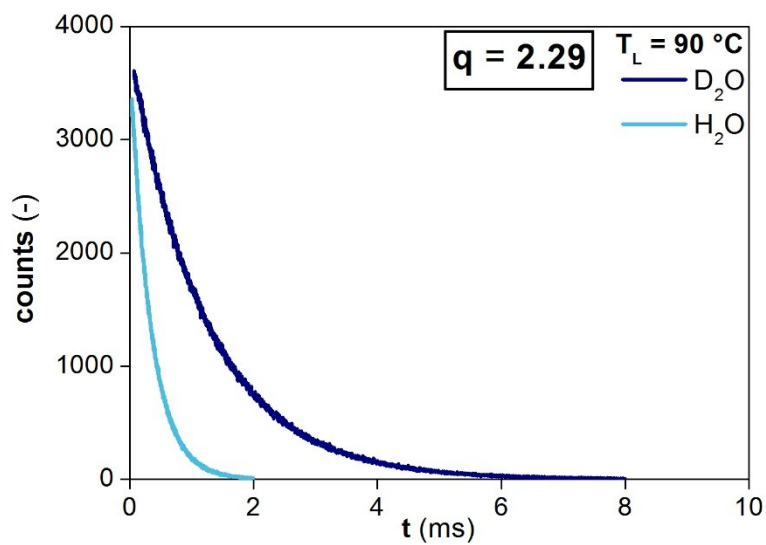


Figure S15– Emission decay curves at room temperature of Eu^{3+} dissolved at 175 °C in D_2O saturated $[\text{Dbet}][\text{Tf}_2\text{N}]$ and H_2O saturated $[\text{Hbet}][\text{Tf}_2\text{N}]$. $q = 2.29$.

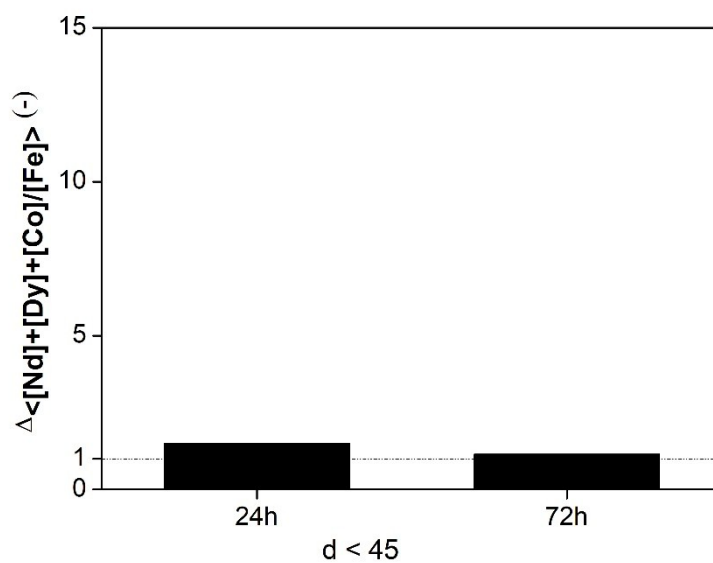


Figure S16 - Relative selectivity of the leaching process for the dross from scrap casting as a function of the time. A reference value of 1 to the initial ratio is pointed out for comparison.

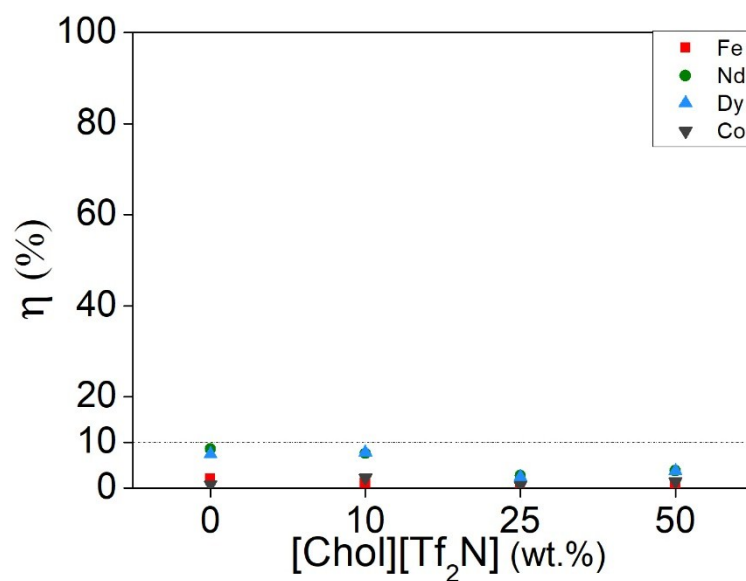


Figure S17 - Recovery efficiency of Fe(III), Nd(III), Dy(III) and Co(II) from leached NdFeB magnets as function of the [Chol][Tf₂N] content (wt.%) in [Hbet][Tf₂N].

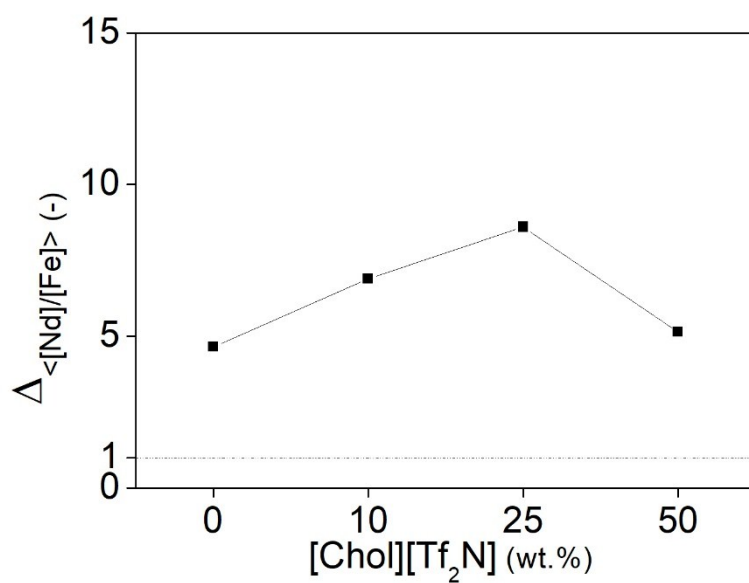


Figure S18- Selectivity of the leaching process for the NdFeB magnets as a function of the [Chol][Tf₂N] content (wt.%), in [Hbet][Tf₂N].